

# Energy Optimal Path Planning of Ocean-energy driven Unmanned Surface Vehicles

Yulei Liao<sup>1,2</sup>, Ke Li<sup>1,2</sup>, Yongbo Zhao<sup>1,2</sup>, Haotian Tang<sup>1,2</sup>, Ming Zhang<sup>1,2\*</sup>, Xiaofeng Liu<sup>1,2</sup>, Zhi-Ming Yuan<sup>3</sup>

1. National Key Laboratory of Autonomous Marine Vehicle Technology, Harbin Engineering University, Harbin 150001, China;

2. Sanya Nanhai Innovation and Development Base of Harbin Engineering University, Sanya, 572000, China;

3. Department of Naval Architecture, Ocean and Marine Engineering, University of Strathclyde, Glasgow, G4 0TD, United Kingdom

## ABSTRACT

Ocean energy driven unmanned surface vehicles (OEDUSV) can realize long-time sea observation tasks with long endurance. Most of the studies on OEDUSV are focused on motion control problem. The path planning problem of OEDUSV has rarely been considered in published literature. To fill this research gap, the present study proposes an energy-optimal global path planning solution, which is then applied to an OEDUSV model Yulang. In order to meet the design requirements of endurance, a dynamic ocean environment model is established. The model applies a grid method and combines with a time-dependent marine environment forecast data. Based on its energy consumption and ocean energy capture model, a Dijkstra based energy optimal global path planning method is then proposed. A Theta\* algorithm is introduced to solve the invalid turning points problem. An original visibility detection algorithm is optimized by introducing a clipping algorithm and an energy consumption function. Under static and dynamic ocean environment conditions, the performance of the energy optimal Theta\* algorithm is compared with that of the energy optimal Dijkstra algorithm, the traditional Dijkstra algorithm and the traditional Theta\* algorithm. The results show that the path planned by the energy-optimal Theta\* algorithm actually consumes the lowest energy.

**Keywords:** Ocean energy-driven unmanned surface vehicle, Theta\* algorithm, Energy optimal algorithm, Global path planning, Ocean energy capture

## 1. Introduction

### 1.1. Background of this study

As marine robotics technology continuously evolves towards autonomy, intelligence, wide-ranging capabilities, and long endurance<sup>[1, 2]</sup>, the issue of conventional marine robots having insufficient self-energy and limited endurance becomes increasingly prominent. Ocean contains a large amount of energy<sup>[3]</sup>. In order to improve the endurance of marine vehicles, many attempts have been made by researchers to integrate ocean energy capture technologies into marine vehicles<sup>[4]</sup>. By developing and utilizing ocean energy to achieve online energy replenishment for marine robots, and thereby enhancing their endurance, this is a hot topic in current marine robotics technology research.<sup>[5-7]</sup> Thus, various styles of Ocean energy driven unmanned surface vehicles (OEDUSV) have emerged.

OEDUSV is a type of marine vehicles that captures ocean energy in a real-time manner to ensure self-sustaining power for several months<sup>[8, 9]</sup>. Currently, OEDUSVs include wave gliders propelled by wave energy, solar unmanned boats powered by photovoltaic power generation, and unmanned sailing boats equipped with wind turbines or sails powered by wind energy and a multi-energy driven robot<sup>[10, 11]</sup>. Most of the studies on OEDUSV are focused on motion control problem. Liao et al. have done research on the control of underwater gliders<sup>[12, 13]</sup>. Zhou et al. have carried out research on control problems in the area of underwater gliders<sup>[14, 15]</sup>. Ma et al. studied the problem of

control of unmanned sailing boats<sup>[16]</sup>. At the same time, global path planning is the core issue of OEDUSV research. Reasonable navigation route scheme will maximize the use of ocean energy, improve its working efficiency and endurance, and complete wide-range and long-term navigation observation and exploration tasks.

## 1.2. Research status of path planning

Global path planning, as the foundation of marine vehicle navigation, has always been a hot topic of research. Most path planning methods aim to minimize distance<sup>[17, 18]</sup>. With the increasing complexity of observation tasks, the time to complete observation missions has increased dramatically. However the amount of initial energy carried by marine vehicles is limited. As a result, marine vehicles are required to have higher endurance capabilities. Energy-saving requirements have become the mainstream of path planning for high endurance marine vehicles. The searched paths that need to be energy-saving to improve the endurance of the marine vehicle. Therefore, the goal of planning the path shifts from optimal distance or time to optimal energy consumption<sup>[19]</sup>.

Cui et al.<sup>[20]</sup> proposed a global path planning algorithm for a USV based on ant colony optimization algorithm. A global path planning model was constructed for the energy consumption cost of USV navigation and steering control, which was iteratively optimized using ant colony algorithm. Li et al.<sup>[21]</sup> used an improved reinforcement learning algorithm to calculate the optimal energy consumption path for a USV considering the influence of ocean currents, and smoothed the path using a B-spline method. Gao et al.<sup>[22]</sup> analyzed the energy transformation and sailing resistance of the USV propulsion systems, established an energy consumption model for the USV, and completed global path planning based on an improved ant colony algorithm. Xuan et al.<sup>[23]</sup> used Tabu Search algorithm to optimize A\* algorithm by filtering strategy, replacing the original local shortest path with the global optimum. It saves energy consumption of unmanned ships and reduces sailing time.

Due to the high endurance task requirements, global path planning of marine vehicle is a type of dynamic planning across time ranges. While the environmental data involved in the above literature is static environmental data, which is difficult to meet the requirements of high-endurance planning. Researchers began to introduce dynamic environmental variables when exploring global path planning of marine vehicle.

Niu et al.<sup>[24]</sup> proposed an energy-saving path planning method for USVs in spatio-temporal variant environments. Edge extension was made for the coastline and Voronoi diagram method and genetic algorithm were adopted to search for energy-saving paths. Zhang et al.<sup>[25]</sup> proposed a distance based dynamic global energy-saving path method for USV. An optimized A\* algorithm was used to search for the optimal path at each node, considering distance cost and changes of ocean data. This improved the endurance of USV and met practical navigation requirements. Wu et al.<sup>[26]</sup> proposed a A\* algorithm for motion planning optimization to simultaneously optimize efficiency, safety, and energy objectives in a dynamic ocean environment, meanwhile satisfying multiple constraint conditions. This can improve planning time, reduce navigation risks, and reduce navigation energy consumption, fully ensuring the efficiency of unmanned underwater vehicles in executing tasks. Lan et al.<sup>[27]</sup> used an improved random search tree algorithm to solve the path planning problem for glider formations in actual ocean current environments, by reducing overly aggressive control strategies such as forced crossing of ocean currents to consume unit energy running time.

Ma et al.<sup>[28]</sup> proposed an improved PSO algorithm considering the impact of ocean currents, which established a model of the energy consumption of ocean currents on OEDUSV. The algorithm fully considered multiple targets such as safety and sailing distance, and the effectiveness of the algorithm was verified by simulation experiments. Jia et al.<sup>[29, 30]</sup> focused on OEDUSV that only consider wind energy capture. They constructed an energy expansion tree for the ocean environment and a wind energy capture model for the robot, which combined the A\* algorithm to solve the path planning problem of OEDUSV in the sea wind field.

From the perspective of energy consumption and marine energy capture, the above research realizes the global path planning of energy conservation in the marine environment. However, the above research has unsolved problems

and limitations. They rely on overly idealized models of the marine environment, assuming steady or linearly environment variances that do not reflect to the actual spatiotemporal variant of the ocean environment. Additionally, they insufficiently consider of energy saving problems. when considering environmental disturbances, the goal is to minimize the sailing distance or time, without considering the process of ocean energy capture. In fact, they incompletely consider the ways of multi-source energy capture. Therefore, the novelty of this article is to study the best global path planning strategy for OEDUSV using multi-source energy capture in dynamic marine environments.

1.3. The objectives of this study

In view of the existing problems in the current OEDUSV path planning research, this paper aims to study the optimal global path planning of energy consumption considering multiple energy captures in the dynamic marine environment. In this paper, Yulang is taken as the research object, and the Theta\*-EOP algorithm is used to study the global path planning. This paper mainly consists of the following parts: Section 2. Introduction to the basic parameters of the Yulang, as well as the energy consumption model and ocean energy capture model. Section 3: Establish a three-dimensional grid ocean environment model, optimize the child node expansion direction, cost function, and child node expansion conditions of the Dijkstra algorithm. Combine the clipping algorithm to optimize the visibility detection part of the Theta\* algorithm, and complete the design of the energy optimal Theta\* global path planning method (Theta\*-EOP). Section 4: Conduct simulation experiments to verify the feasibility and effectiveness of Dijkstra EOP and Theta\*-EOP. Figure 1 is the graphical abstract of this study.

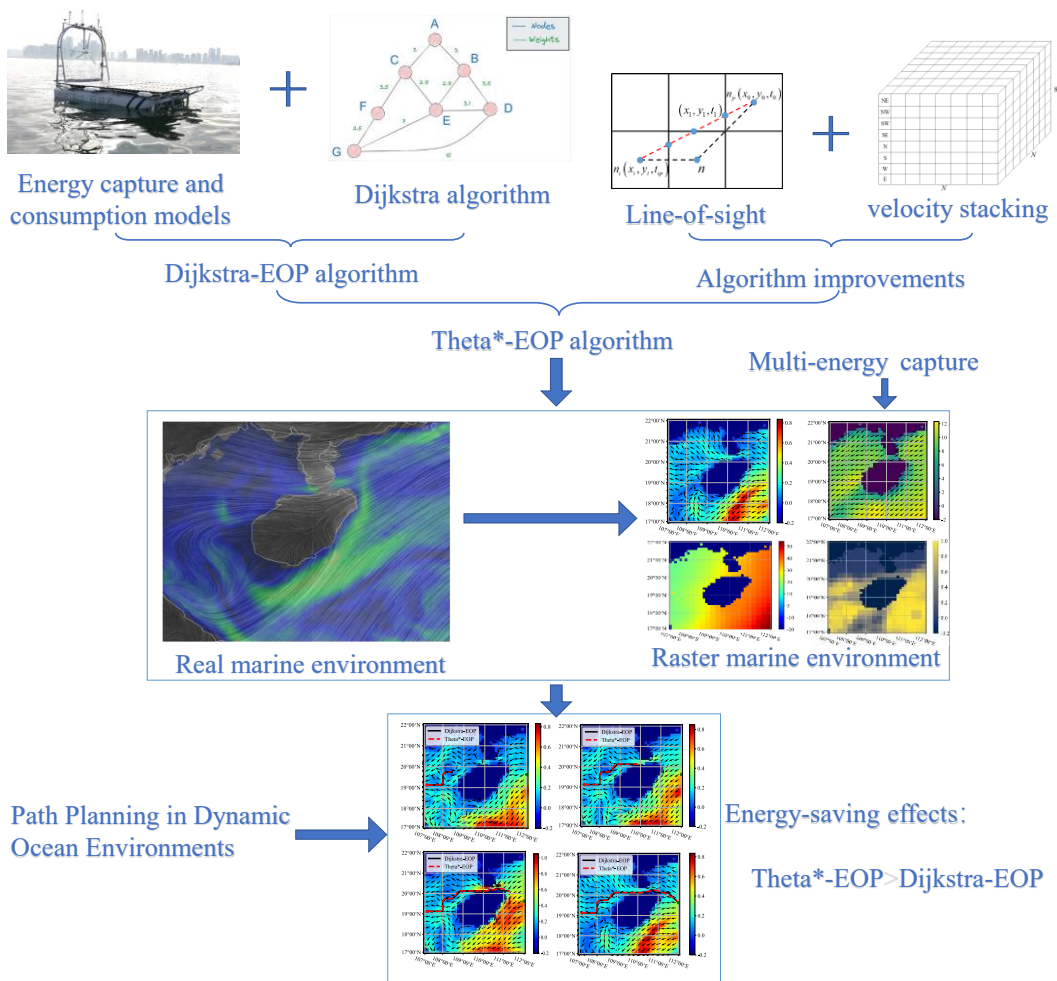


Fig. 1. Graphical abstract of this study

## 2. Energy consumption model for OEDUSV

### 2.1. Design of Yulang

In this paper, the OEDUSV *Yulang* is taken as a target vehicle<sup>[31, 32]</sup>, as shown in Figure 2. The main technical indicators are shown in Table 1. *Yulang* can monitor ocean environment information such as ocean currents, sea wind and light intensity through a variety of ocean environment sensors, and can also use ocean energy such as solar energy and wind energy through energy capture equipment to improve its endurance.

The weather station, current meter, light intensity and other sensor modules carried by the *Yulang* can respectively monitor the scale and direction of the sea wind encountered during navigation, the scale and direction of the ocean current, and the intensity of the light. Wind power generation modules and photovoltaic panels can convert wind and solar energy into electricity stored in battery modules. The vision sensor module can provide the information of obstacles in front of the *Yulang*, and the integrated navigation module can provide the position, speed and heading information for navigation.



Fig. 2. The OEDUSV *Yulang* in Zhanjiang in 2021.

Table 1

Main design particulars of the *Yulang*

parameter	numerical value
Length over all, $L_{OA}$	5.08m
Length between perpendiculars, $L_{PP}$	4.50m
Extreme breadth	3.20m
Moulded breadth	2.81m
Air draft	3.35m
Moulded draft	0.3m
Displacement	498kg

### 2.2. Energy consumption model

Li and Liao et al.<sup>[33, 34]</sup> proposed that the energy is mainly consumed by the control system and power system, and ocean energy is mainly captured by wind turbine power generation modules and photovoltaic panels. The total energy consumption during navigation can be expressed as:

$$E = E_1 + E_2 - E_3 = (P_1 + P_2 + P_3 - P_4 - P_5) \frac{L}{|V_{OEDUSV}|} \quad (1)$$

where  $E_1$  is the total energy consumption of the control system,  $E_2$  is the total energy consumption of the power system,  $E_3$  is the energy capture amount,  $P_1$  is the total power of the control system,  $P_2$  is the servo power,  $P_3$  is the

propeller power,  $P_4$  is the power generation of the wind turbine,  $P_5$  is the power generation of the photovoltaic panel,  $L$  is the sailing distance, and  $|V_{OEDUSV}|$  is the speed of the robot.

Li and Liao et al.<sup>[33]</sup>, the energy consumption of the *Yulang* mainly comes from the energy consumption of various sensors in the control system, as well as the energy consumption of the servo and thrusters in the power system. Li and Liao et al.<sup>[33, 34]</sup> proposed that it can be concluded that the energy consumption model and power system energy consumption under the influence of ocean currents and winds, as well as the total energy consumption model of the *Yulang* during navigation, are:

$$\begin{cases} E_1 + E_2 = (P_1 + P_2) \frac{L}{|V_{OEDUSV}|} + E_{cur} + E_{wind} \\ E_{cur} = 23.177 \cdot |V_{OEDUSV \rightarrow cur}|^3 \cdot \cos^2 \psi_{rc} \cdot \frac{L}{|V_{OEDUSV}|} \\ E_{wind} = 0.235 \cdot |V_{OEDUSV \rightarrow wind}|^3 \cdot \cos^2 \psi_{rw} \cdot \frac{L}{|V_{OEDUSV}|} \end{cases} \quad (2)$$

where  $E_{cur}$  represents the energy consumption of the *Yulang*'s power system considering the influence of ocean currents;  $E_{wind}$  is the energy consumption of the *Yulang*'s power system considering the influence of sea wind;  $V_{OEDUSV \rightarrow cur}$  is the velocity vector of the robot relative to the ocean current;  $\psi_{rc}$  is the angle of attack;  $V_{OEDUSV \rightarrow wind}$  is the velocity vector of the *Yulang* relative to the sea wind;  $\psi_{rw}$  is the wind direction angle.

Combined with the literature, the energy capture model of sea wind and solar energy can be expressed as follows:

$$E_3 = (P_4 + P_5) \frac{L}{|V_{OEDUSV}|} = E_w + E_s \quad (3)$$

where  $E_w$  represents the wind energy captured by the *Yulang*,  $E_s$  is the solar energy captured by the robot.

### 3. Energy optimal global path planning method for OEDUSV

In this chapter, the optimal energy path planning method is designed according to the characteristics of OEDUSV (*Yulang*). This method takes advantage of the characteristics of OEDUSV that can capture ocean energy and search for the path with the lowest total energy consumption. This method improves the endurance of OEDUSV and ensures that it can complete large-range and long-endurance observation tasks.

#### 3.1. Construction of a three-dimensional raster ocean environment model

Ocean environment forecasting technology can provide accurate real-time variant information of ocean environment, and path planning optimization can be achieved by using ocean environment forecasting data<sup>[35, 36]</sup>. Wind and ocean currents affect wind capture and energy consumption. Solar radiation and atmospheric clouds affect solar capture. Therefore, combining the forecast data of ocean current and sea wind provided by the Global Operational Real-Time Ocean Forecast System (RTOFS)<sup>[37]</sup>, Solar radiation and cloud forecast data provided by the European Centre for Medium-Range Weather Forecasts (ECMWF)<sup>[35, 36]</sup> are used to build a grid model of the ocean environment.

In this paper, we take a scenario that the *Yulang* conducts sea surface observation mission around Hainan Province, and obtain dynamic dataset of sea wind, ocean current, solar radiation and atmospheric clouds in the region

of longitude from East 107° to East 112° and latitude from North 17° to North 22° on a day in November 2021. Set the resolution of the grid map as 40×40, with each grid representing 14.0km of actual geography. Figure 3 shows ocean current environment models. The directions of arrows represent the directions of ocean currents (unit: °) and colors of contours represent the scales of ocean currents (unit: m/s). Figure 4 shows the sea wind environment model at different moments. The directions and colors of arrows in Figure 4 are similar to those of Figure 3. Figure 5 shows the solar radiation, and the colors represent the solar radiation intensity of the ocean surface under the clear sky (unit: W/m<sup>2</sup>); Figure 6 shows the atmospheric cloud environment model, and the color represents atmospheric cloud transmittance.

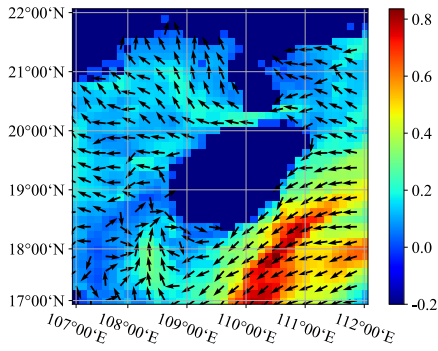


**Fig .3.** Current model

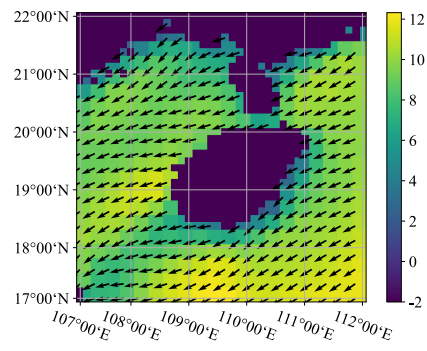


**Fig .4.** Sea wind model

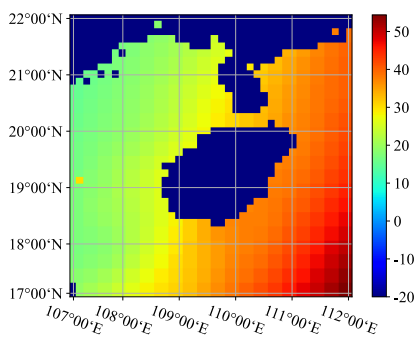


**Fig .5.** Solar radiation model

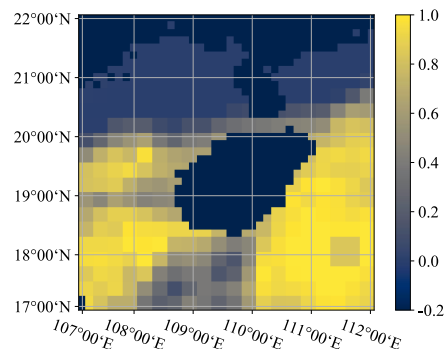


**Fig .6.** Atmospheric cloud model

Ocean currents, sea winds, solar radiation, atmospheric clouds, and other ocean environments not only are spatial-distributed, however also are time-variant. In order to study the variance of ocean environment over time and expand the dimensions of the grid model, time is used as an additional dimension to establish a three-dimensional grid ocean environment model as shown in Figure 7. The nodes in the grid model are renumbered using a three-dimensional Cartesian coordinate.

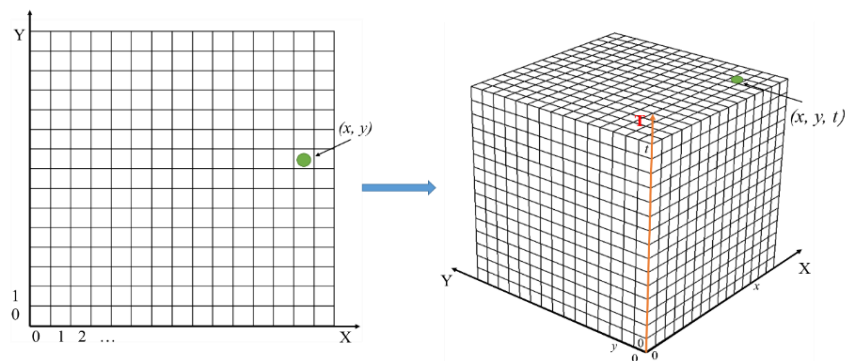


**Fig .7.** 3D Grid Ocean Environment Model

The horizontal plane is the  $X$ - $Y$  axis frame representing the position of each node in the spatial grid model; The vertical direction is the  $T$ -axis, representing the time series of each node. Node  $(x, y, t)$  can not only store obstacle information at position  $(x, y)$ , however also store data including environment information of position  $(x, y)$  at time step  $t$ .

### 3.2. Design of Dijkstra Global Path Planning Method for Energy Optimization

In order to complete the energy optimal global path planning method, this section will improve the child node expansion direction, cost function, and child node expansion conditions of the Dijkstra algorithm, and propose the energy optimal Dijkstra Global Path Planning Method (Dijkstra EOP). The Dijkstra algorithm was chosen because it always finds the best path for cost. However, due to the cost-optimal characteristics of the Dijkstra algorithm, Dijkstra needs to search for a large number of points, resulting in a complex calculation process, long time and low efficiency. And, there may be invalid turn points in the path searched out by Dijkstra, which will be improved in section 3.3.

#### (1) Extension direction of child nodes in a three-dimensional grid ocean environment model

In the three-dimensional grid ocean environment model, when the *Yulang* expands from the current node  $n(x_n, y_n, t_n)$  to child nodes in eight directions of extension. Due to the different distances of the extension, the time to extend in the eight directions is also different. The eight directions will no longer be extended in the horizontal plane, however in the three-dimensional coordinate, as shown in Figure 8.

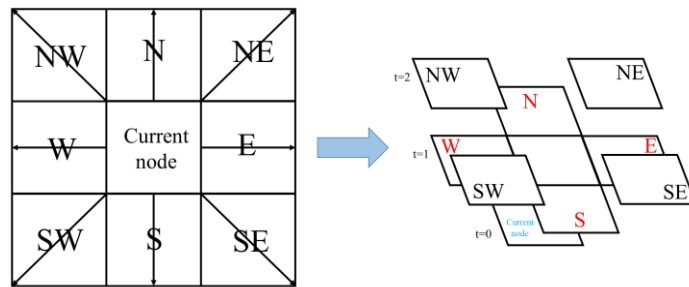


**Fig.8.** Node Expansion Direction under 3D Grid Model

In each process of expanding nodes, the ocean current velocity  $V_{cur}$  and sea wind velocity  $V_{wind}$  at node  $n(x_n, y_n)$  are fixed. Therefore, there are eight feasible solutions for the relative ocean current velocity  $V_{OEDUSV \rightarrow cur}$

and relative sea wind velocity  $V_{OEDUSV \rightarrow wind}$  of the *Yulang* at the current node based on the eight extended heading.

For the convenience of discussing these velocities, this paper introduces the concept of velocity stack<sup>[17]</sup>, whose structure is shown in Figure 9. From the bottom layer to the top layer, each layer represents the expansion direction of due east (E), due west (W), due north (N), due south (S), northeast (NE), southeast (SE), northwest (NW), and southwest (SW). Each layer stores the relative current velocity and relative sea wind velocity of the *Yulang* that expands from the current point in the direction of the label. Each column represents a node in the raster map of  $N \times N$ .  $N$  represents the size of the raster maps. However, due to the fact that the magnitude and direction of ocean currents and winds vary over time when expanding child nodes, the impact of time needs to be considered when determining the accessibility of sub nodes. Meanwhile, considering the time effectiveness of ocean environment forecast data, the time dimension has the maximum value  $t_{max}$  in the three-dimensional grid ocean environmental model.  $t_n$  is the

time from the start point to point  $n(x_n, y_n)$ , regardless of the size  $N \times N$  of the map. When  $t_n > t_{max}$ , the ocean environment forecast data loses its time effectiveness and the algorithm search fails. The algorithm should search based on the new forecast data.

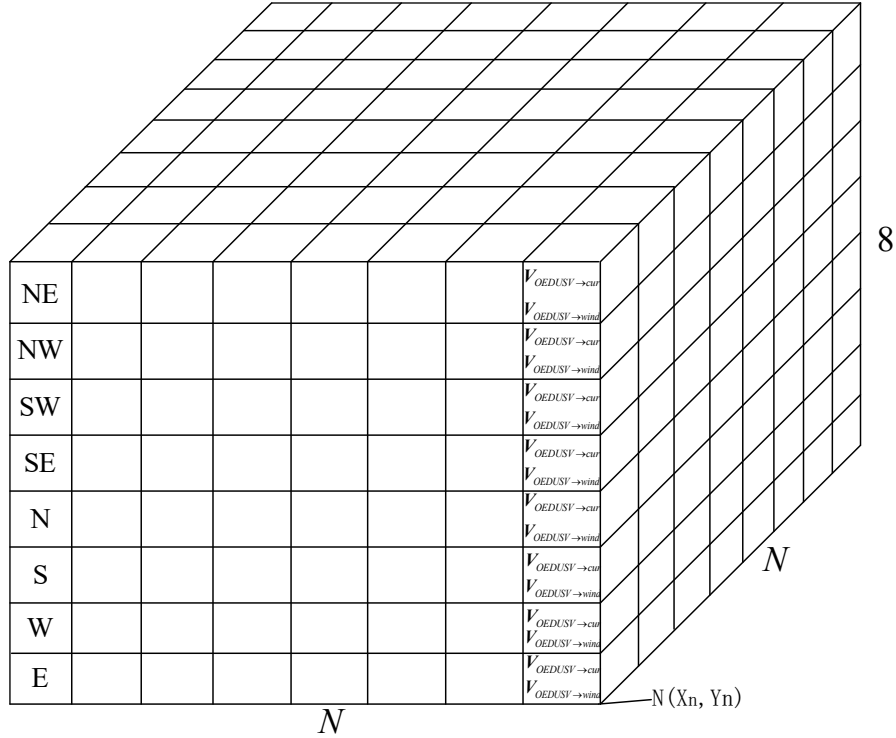


Fig . 9. Concept of Velocity Stack

### (2) Energy consumption cost function based on energy consumption model

Based on the velocity stack and the energy consumption model of the *Yulang*, the energy consumption can be calculated when the current node expands to child nodes, as shown in Equations (4) and (5). The goal of the energy optimal global path planning research for the *Yulang* is to save energy and improve endurance. Therefore, when using a Theta\* algorithm to search paths, the energy consumption calculated using formulas (4) and (5) is used as the proxy value.

$$e_n(x_i, y_i) = (E_{cur} + E_{wind} + P_1 + P_2) \cdot \frac{d_m^j}{|V_{OEDUSV}|} \quad (4)$$

$$e(x_i, y_i) = e_n(x_i, y_i) + e(x_n, y_n) \quad (5)$$

where  $(x_n, y_n)$  represents the current node  $n$ ;  $(x_i, y_i)$  represents the child node  $i$  of node  $n$ .  $i$  is integral and  $i \in [1, 8]$ ;  $e_n(x_i, y_i)$  represents the energy consumption generated by navigating from the current node  $n$  to the child node  $i$ ;  $e(x_n, y_n)$  represents the total energy consumption generated from the starting point of navigation to the current node  $n$ ;  $e(x_i, y_i)$  represents the total energy consumption generated by sailing from the starting point through the current node  $n$  to the child node  $i$ ;  $N_{layer}$  represents the number of layers at which the velocity is located;  $d$  represents the unit distance cost from the current node  $n$  to the child node  $i$ .  $j$  represents the number of layers. When  $j=1, 2, 3, 4$ ,  $d_m^j = d$ ; When  $j=5, 6, 7, 8$ ,  $d_m^j = \sqrt{2}d$ .

### (3) Extension conditions of child nodes under the influence of ocean environment

Equation (4) can be used to calculate the energy consumed by the influence of ocean currents and winds of the *Yulang* during navigation process, However, the propeller power of the *Yulang* is limited. If energy consumption is

excessive, the propeller will not be able to provide the required power. The *Yulang* will not be able to reach these child nodes through the current node. In order to accelerate the search speed of Theta\* algorithm, these child nodes are set as unreachable nodes, and Equation (4) is rewritten as Equation (6).

$$e_n(x_i, y_i) = \begin{cases} e_n(x_i, y_i), & e_n(x_i, y_i) < P_{MAX} \frac{d_m^j}{|V_{OEDUSV}|} \\ \infty, & e_n(x_i, y_i) \geq P_{MAX} \frac{d_m^j}{|V_{OEDUSV}|} \end{cases} \quad (6)$$

where  $P_{MAX}$  is the maximum power of the propeller. When the Theta\* algorithm is in progress, regarding the expansion conditions of child nodes and the cost function based on the energy consumption model, an energy-saving path can be obtained from the starting point to the target point. However, in order to obtain the optimal path for energy, it is also necessary to consider the ocean energy capture of the *Yulang*.

#### (4) Energy capture cost function based on ocean energy capture model

The energy optimal global path planning of the *Yulang* not only considers the impact of ocean currents and winds on energy consumption, however also considers the ocean energy that can be captured during navigation process. The ocean energy captured by the *Yulang* is calculated by combining the velocity stack and ocean energy capture model, as shown in Equations (7) and (8).

$$e_{n \rightarrow cap}(x_i, y_i) = P_4 \cdot \frac{d_m^j}{|V_{OEDUSV}|} + P_5 \cdot \frac{d_m^j}{|V_{OEDUSV}|} \quad (7)$$

$$e_{cap}(x_i, y_i) = e_{n \rightarrow cap}(x_i, y_i) + e_{cap}(x_{cur}, y_{cur}) \quad (8)$$

where  $e_{n \rightarrow cap}(x_i, y_i)$  represents the ocean energy that can be captured from the current node  $n$  to the child node  $i$ ;  $e_{cap}(x_{cur}, y_{cur})$  represents the ocean energy captured by the *Yulang* from the starting point to the current node  $n$ ;  $e_{cap}(x_i, y_i)$  represents the ocean energy captured by the *Yulang* from the starting point, passing through the node  $n$ , to the child node  $i$ .

Substituting Equations (7) and (8) to Equation (6), the Theta\* algorithm can represent the cost value from the current node to the child node during the search process as shown Equation (9).

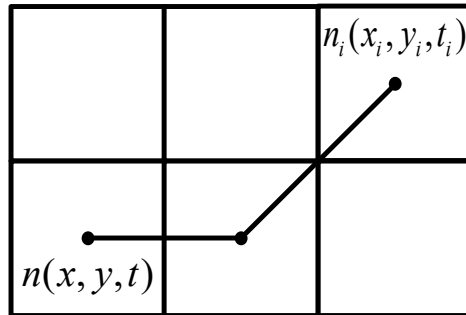
$$e_n(x_i, y_i) = \begin{cases} (E_{cur} + E_{wind} + P_1 + P_2 - P_4 - P_5) \cdot \frac{d_m^j}{|V_{OEDUSV}|}, & e_n(x_i, y_i) < P_{MAX} \frac{d_m^j}{|V_{OEDUSV}|} \\ \infty, & e_n(x_i, y_i) \geq P_{MAX} \frac{d_m^j}{|V_{OEDUSV}|} \end{cases} \quad (9)$$

### 3.3. Design of Theta\* Global Path Planning Method for Energy Optimization

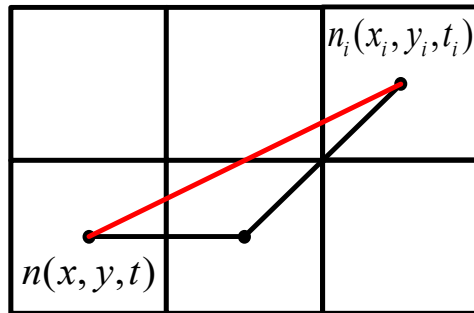
This paper introduces a Theta\* algorithm to solve the problem of limited expansion direction of child nodes in the Dijkstra algorithm, and completes the design of the energy optimal Theta\* global path planning method (Theta\*-EOP). The child node expansion directions in the Dijkstra algorithm only exist in 8 possible directions spaced at 45° intervals from 0-360°, as shown in Figure 10(a). The Theta\* algorithm combines the characteristics of the Visibility Graph (VG) and adds a line-of-sight accessibility detection algorithm on the basis of the Dijkstra algorithm to break through the limitation of the expansion direction of child nodes in the grid environment. It realizes the arbitrary turning angle of the path planning to find the optimal path, as shown in Figure 10(b).

Line-of-sight accessibility detection algorithm requires that when a node  $n(x_n, y_n, t_n)$  is expanded, the

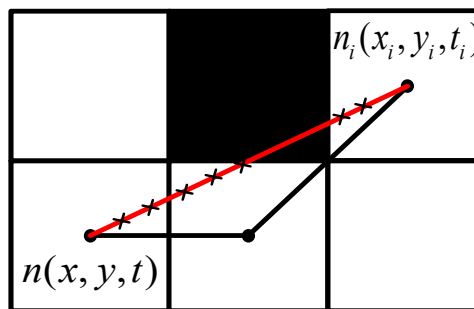
previous node  $n_p(x_0, y_0, t_0)$  of the current node and the next node  $n_i(x_i, y_i, t_i)$  that is about to be expanded are checked for visibility, and if the connection between the two nodes does not pass-through obstacles, it is considered visual. When the accessibility detection results in a three-dimensional grid ocean environment model are visual, the Cohen-Sutherland clipping algorithm is introduced. The Cohen-Sutherland clipping algorithm calculates the coordinates of the intersection of a line segment consisting of any two points on a plane and the edge of the mesh. When the line of sight passes through the mesh, the resulting path length is calculated from the coordinates of the intersection and the edge of the mesh. When using the visibility detection algorithm to calculate the visibility between the parent node  $n_p(x_0, y_0, t_0)$  and the child node  $n_i(x_i, y_i, t_i)$  of the current node  $n(x_n, y_n, t_n)$ , coordinates of the intersection point  $n_1(x_1, y_1, t_1)$  between the line of sight and the grid edge obtained by the Cohen Sutherland cropping algorithm are three-dimensional coordinates. When the line of sight passes through an obstacle, the path generated by the line-of-sight method is invalid, as shown in Figure 10(c).



(a) The limited expansion directions of the Dijkstra algorithm



(b) The path improved by applying line-of-sight detection in the Theta\* algorithm



(c) Paths planned by the Theta\* algorithm that are not traversable

**Fig. 10. Advantages and limitations of the Theta\* algorithm**

When the line of sight passes through a grid centered on  $n_p(x_0, y_0, t_0)$ , additionally calculating the coordinate  $(x_1, y_1)$ , it is necessary to calculate the time  $t_1$  of the line of sight reaching  $(x_1, y_1)$  based on the length of the line of sight, the velocity of the *Yulang* ship, and  $t_0$ . The time  $t_{ip}$  of the line of sight reaching  $(x_i, y_i)$  is required to be calculated, the coordinates  $n_i(x_i, y_i, t_i) \rightarrow n_i(x_i, y_i, t_{ip})$  of the child nodes are updated, and the ocean environment

data of each node in the three-dimensional grid ocean environment model are obtained.

Then, calculate the energy consumption generated when the line of sight passes through any grid. Meanwhile, based on the calculated energy consumption, judge whether the power required for the line of sight to pass through the grid is greater than the maximum power of propeller. If the power required is greater than the maximum power of propeller, the path is invalid.

Theta\*-EOP has been improved on the basis of Dijkstra to realize the arbitrariness of the path turning angle, so as to find the arbitrary path. Although the computational complexity and computation time of Theta\*-EOP still do not achieve very satisfactory results, its computation time is much smaller than the interval between environmental forecast data updates, therefore Theta\*-EOP can be used as the final path planning algorithm.

$$e_0(x_i, y_i, t_i) = \begin{cases} (E_{cur} + E_{wind} + P_1 + P_2 - P_4 - P_5) \cdot \frac{d_0}{|V_{OEDUSV}|} & , e_0(x_i, y_i, t_i) < P_{MAX} \frac{d_0}{|V_{OEDUSV}|} \\ \infty & , e_0(x_i, y_i, t_i) > P_{MAX} \frac{d_0}{|V_{OEDUSV}|} \end{cases} \quad (10)$$

The specific process of the modified visibility detection algorithm is shown in Figure 11.

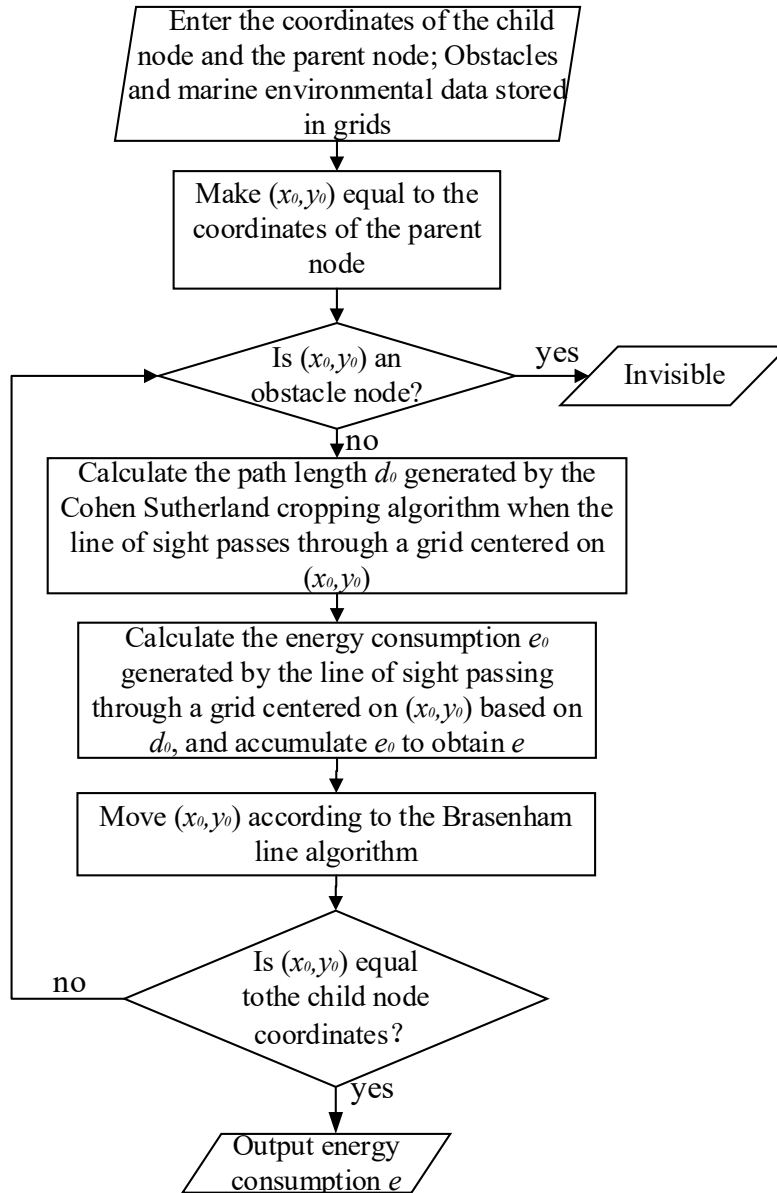


Fig. 11. Flow of line-of-sight accessibility detection algorithm

3.4. Process of Energy Optimal Global Path Planning Method

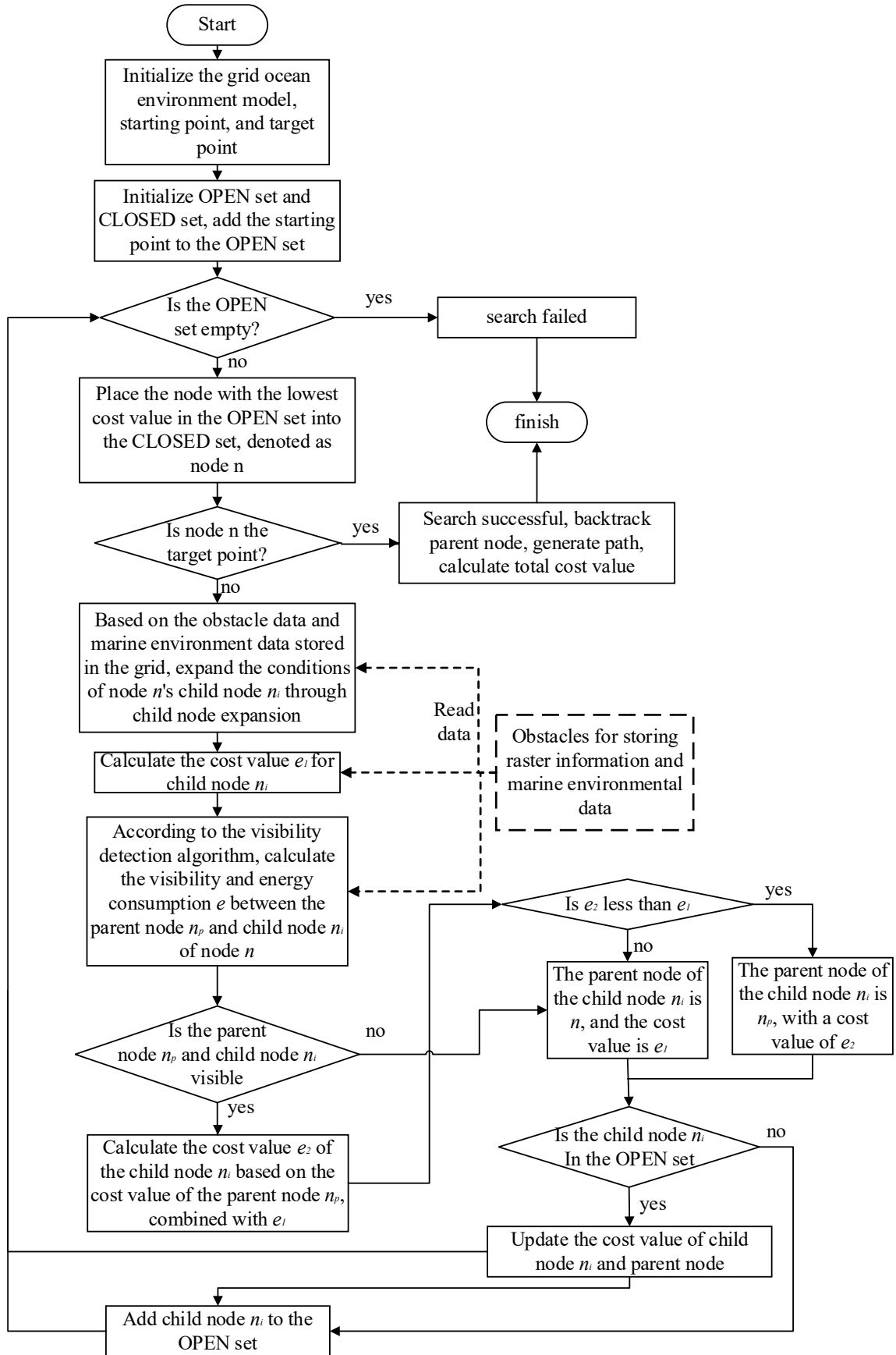


Fig .12. Process flow of energy optimal global path planning method based on the Theta\* algorithm

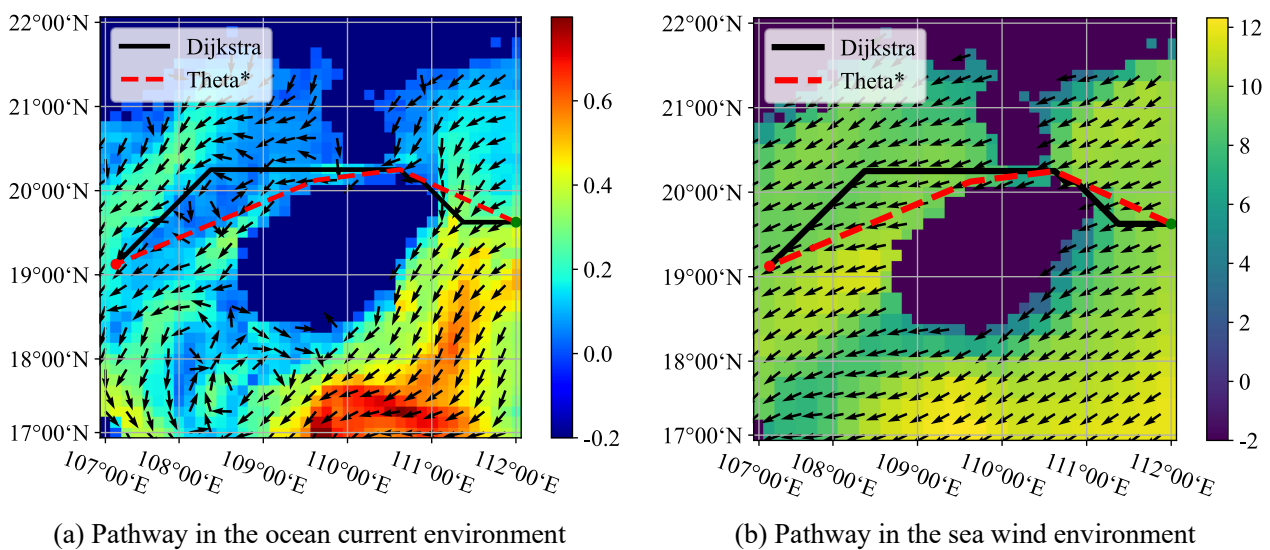
Theta\*-EOP method is applied to demonstrate the process of energy optimal global path planning. The flowchart is shown as Figure 12. In Figure 12, OPEN set represents the set of child nodes that will be expanded, CLOSE set represents the set of child nodes that have already been expanded, and cost value represents the evaluation value from the starting point to the current point, which corresponds to  $e_{cap}(x_i, y_i)$  in the formula (8) in the text. This flowchart illustrates the methodology used in this study and consists of five parts. First, raster processing of marine data is conducted to initialize the starting point and the destination; secondly, select the target node from the OPEN set and expand its child nodes; thirdly, calculate the cost value of the child nodes and perform line-of-sight detection; fourthly, based on the line-of-sight detection results, replace the parent node of the child nodes and ultimately add the child nodes to the OPEN set; fifthly, repeat the process from step two to step five until the destination is reached.

#### 4. Simulation comparison test and analysis

In order to verify the feasibility and effectiveness of the Theta\*-EOP method, simulation experiments are compared with a traditional Dijkstra method, a traditional Theta\* method, and a Dijkstra EOP method as reference groups. Two types of ocean environment models, static and dynamic, are set up for simulation verification. Due to intellectual property protection, the code in this article cannot be open source for the time being.

##### 4.1. Simulation experiment of static ocean environment

Set the resolution of the grid map as  $40 \times 40$ , with each grid representing 14.0km of actual geography. The red dots represent the starting points of the path, and the green dots represent the target points. Based on the ocean environment model established, initial ocean data of the model are selected to simulate a static ocean environment model, and simulation experiments are implemented based on the traditional Dijkstra method, the traditional Theta\* method, the Dijkstra EOP method, and the Theta\*-EOP method. The results of traditional global path planning methods (the former two methods) are shown in Figure 12, the results of energy optimal global path planning methods (the latter two methods) are shown in Figure 13, and the comparison results of the four methods are shown in Table 2.



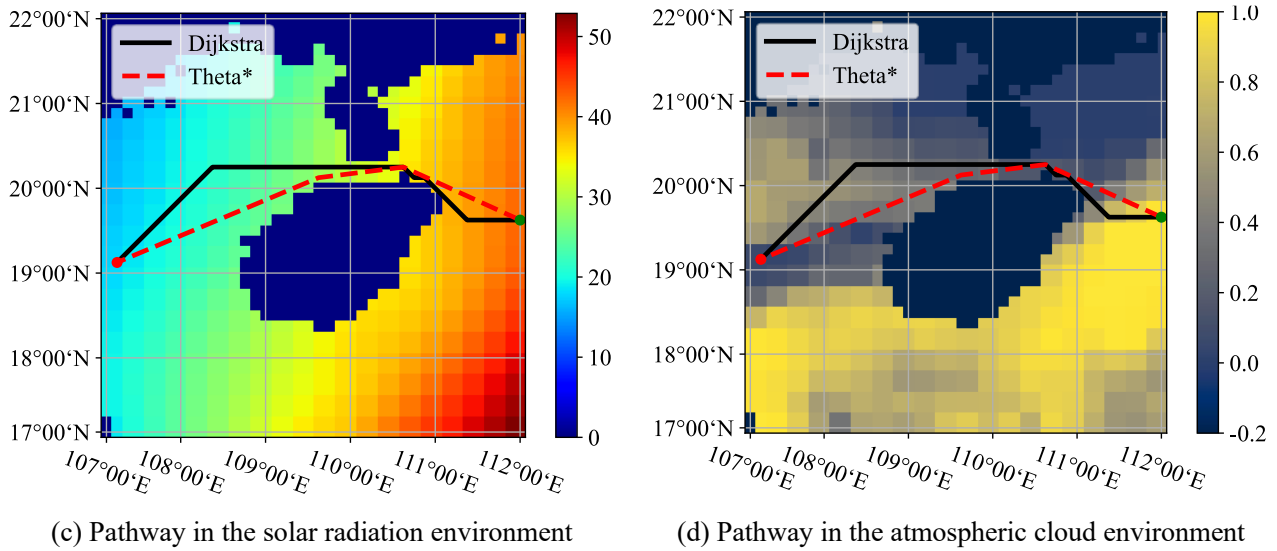


**Fig .13.** Traditional global path planning method

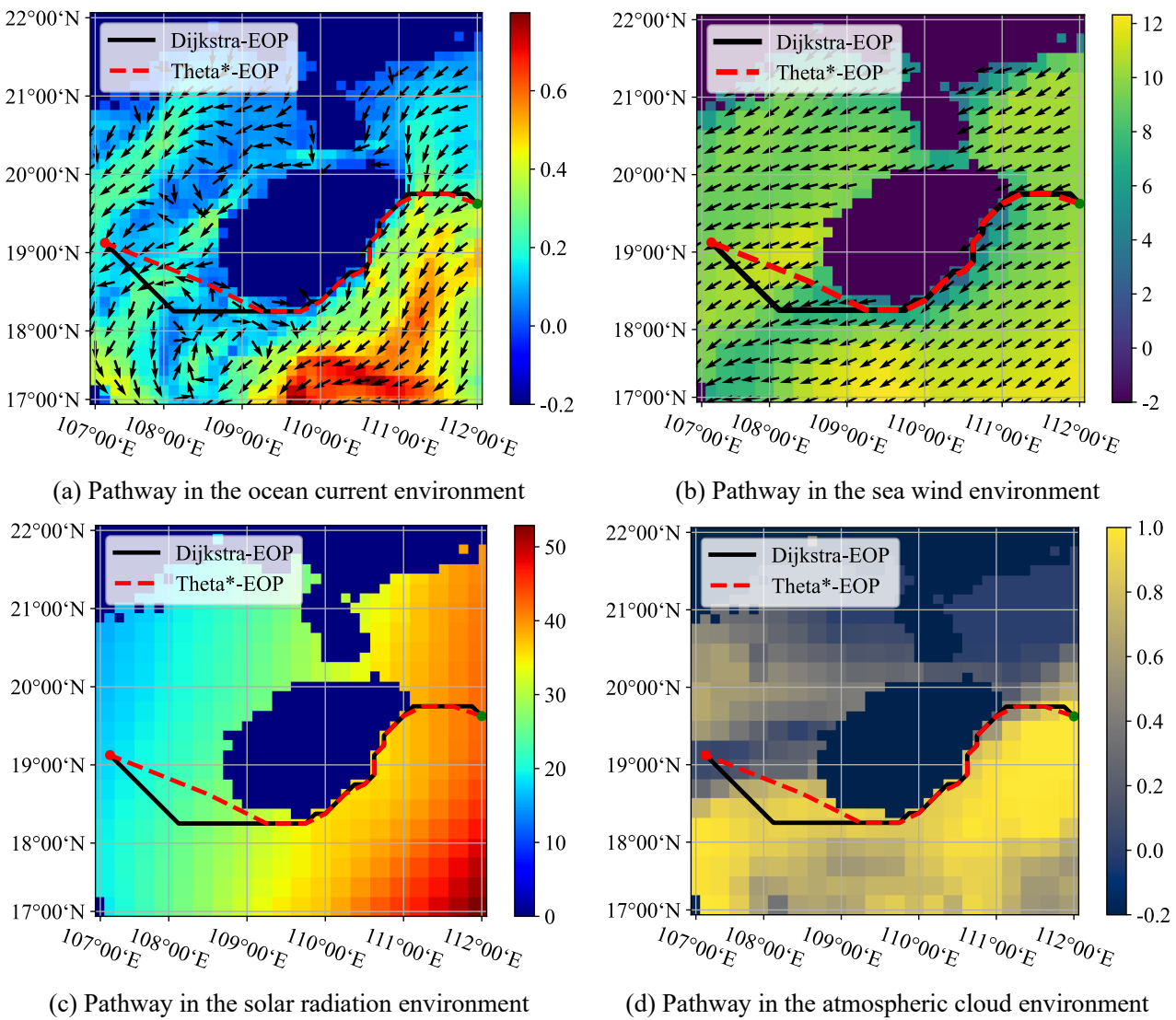


**Fig .14.** Energy optimal global path planning method

**Table 2**

Comparison of simulation results in static ocean environment

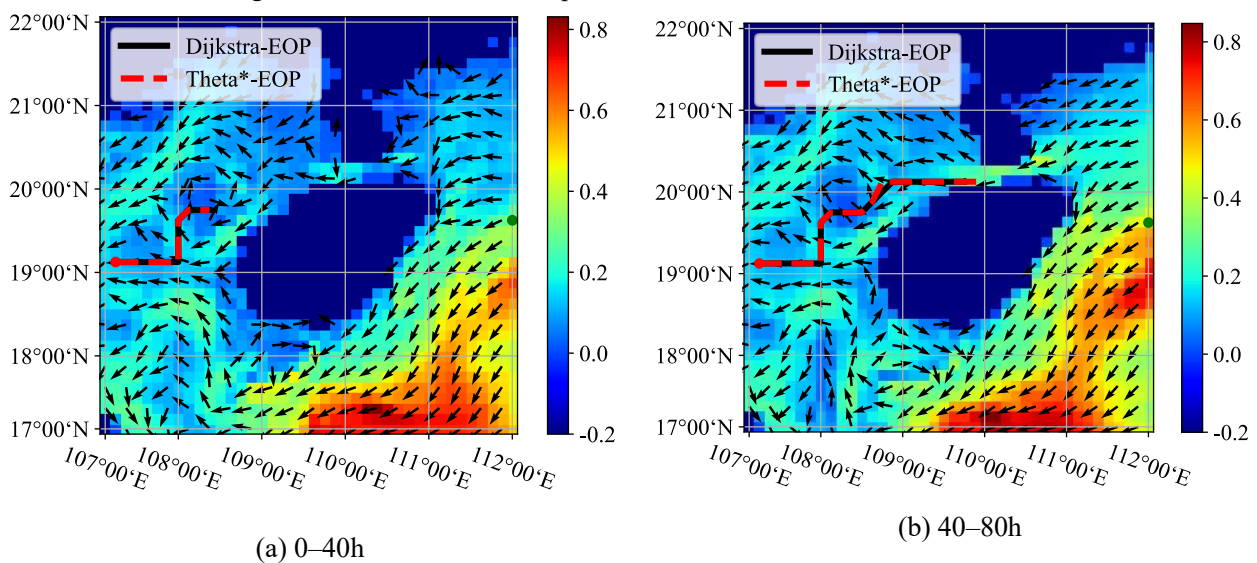
Method	Path length (km)	Ocean capture capacity ( $\times 10^6\text{J}$ )	Total energy consumption ( $\times 10^6\text{J}$ )	Actual total energy consumption ( $\times 10^6\text{J}$ )	Navigation duration (h)	Energy consumption proportion (%)
Dijkstra	613.19	11.47	41.66	30.19	141.94	100.00
Dijkstra-EOP	621.39	11.71	37.45	25.74	143.84	85.26
Theta*	570.65	10.65	36.64	25.99	132.10	86.09
Theta*-EOP	582.68	10.66	35.39	24.73	134.87	81.91

In a static ocean environment, The actual energy consumption of the Dijkstra EOP method (the total energy consumption minus the ocean energy capture is recorded as the actual energy consumption) is lower than the actual energy consumption of the traditional Dijkstra method, The ratio of energy consumption (based on the actual total energy consumption obtained by the traditional Dijkstra method, and the ratio of the actual total energy consumption obtained by other methods to it is recorded as the proportion of energy consumption) has decreased by 14.74%; The actual energy consumption of Theta\*-EOP method is lower than that of traditional Theta\* method, and the ratio of energy consumption is reduced by 4.18%; The actual energy consumption of Theta\*-EOP method is lower than that of Dijkstra EOP method, with a decrease of 3.35% in energy consumption.

Based on the above experimental data, The designed Dijkstra EOP method and Theta\*- EOP method can effectively consider the energy consumption model, ocean energy capture model, and global ocean environment data of the *Yulang*. The methods fully consider the impact of complex ocean environments on the energy consumption and ocean energy capture of the *Yulang*, and can plan a path with less energy consumption compared to the traditional global path planning methods. Meanwhile, from the point of view of the actual total energy consumption during the voyage, the Theta\*-EOP method has the best energy saving performance.

#### 4.2. Simulation experiments in dynamic ocean environments

When implementing global planning under the dynamic environment, ocean current, sea wind, solar radiation, and atmospheric cloud forecast data are updated every 3 hours. The results of the energy optimal global path planning method are shown in Figures 15 to 18, and the comparison results of the four methods are shown in Table 3.



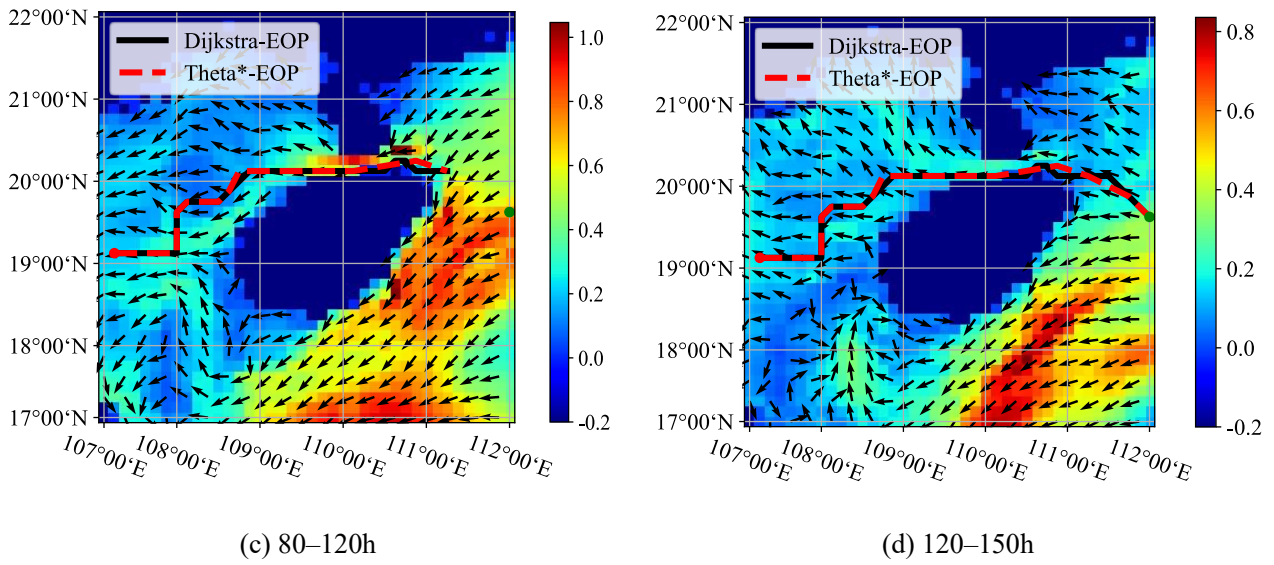


Fig. 15. Pathway in ocean current environment

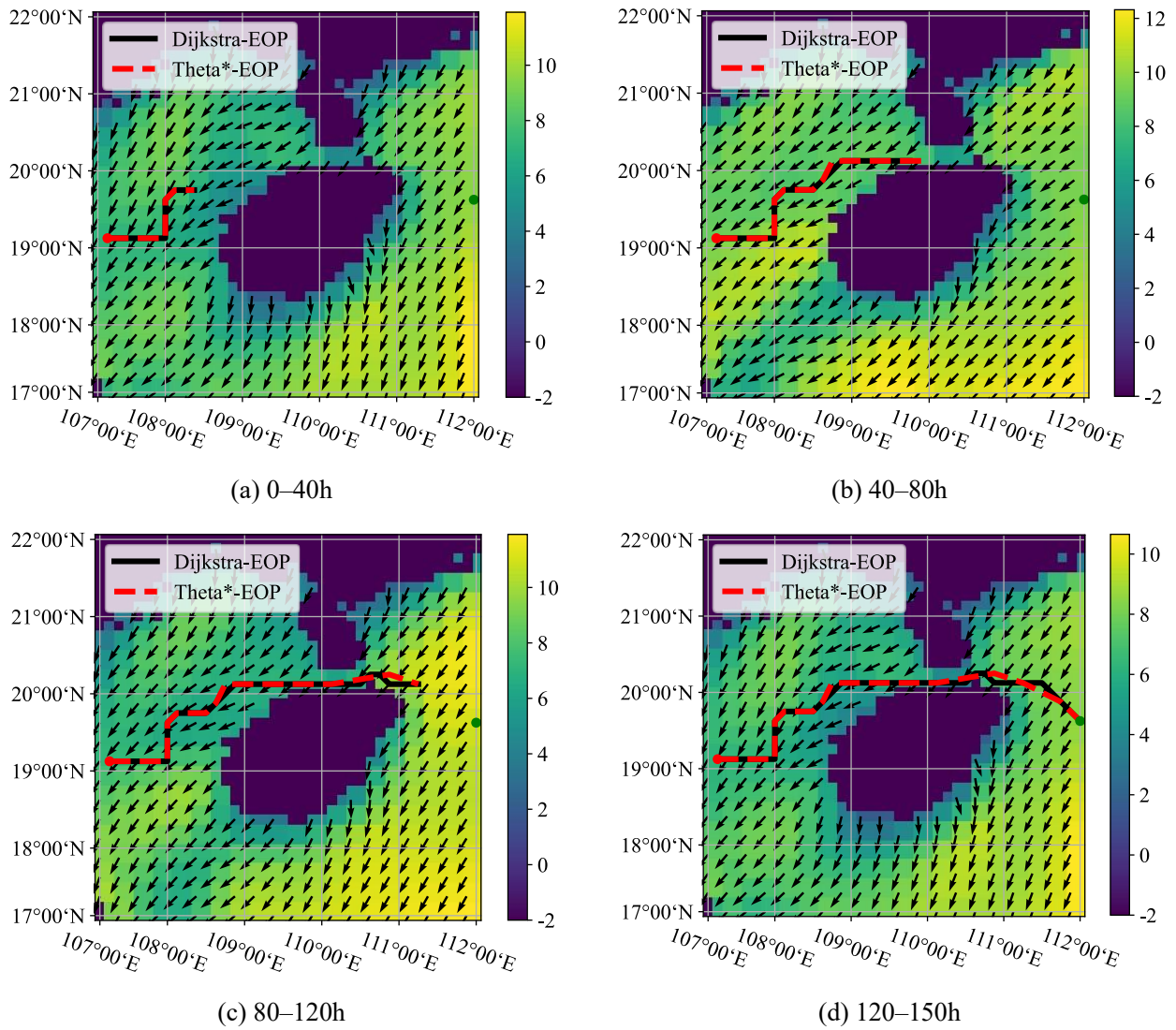
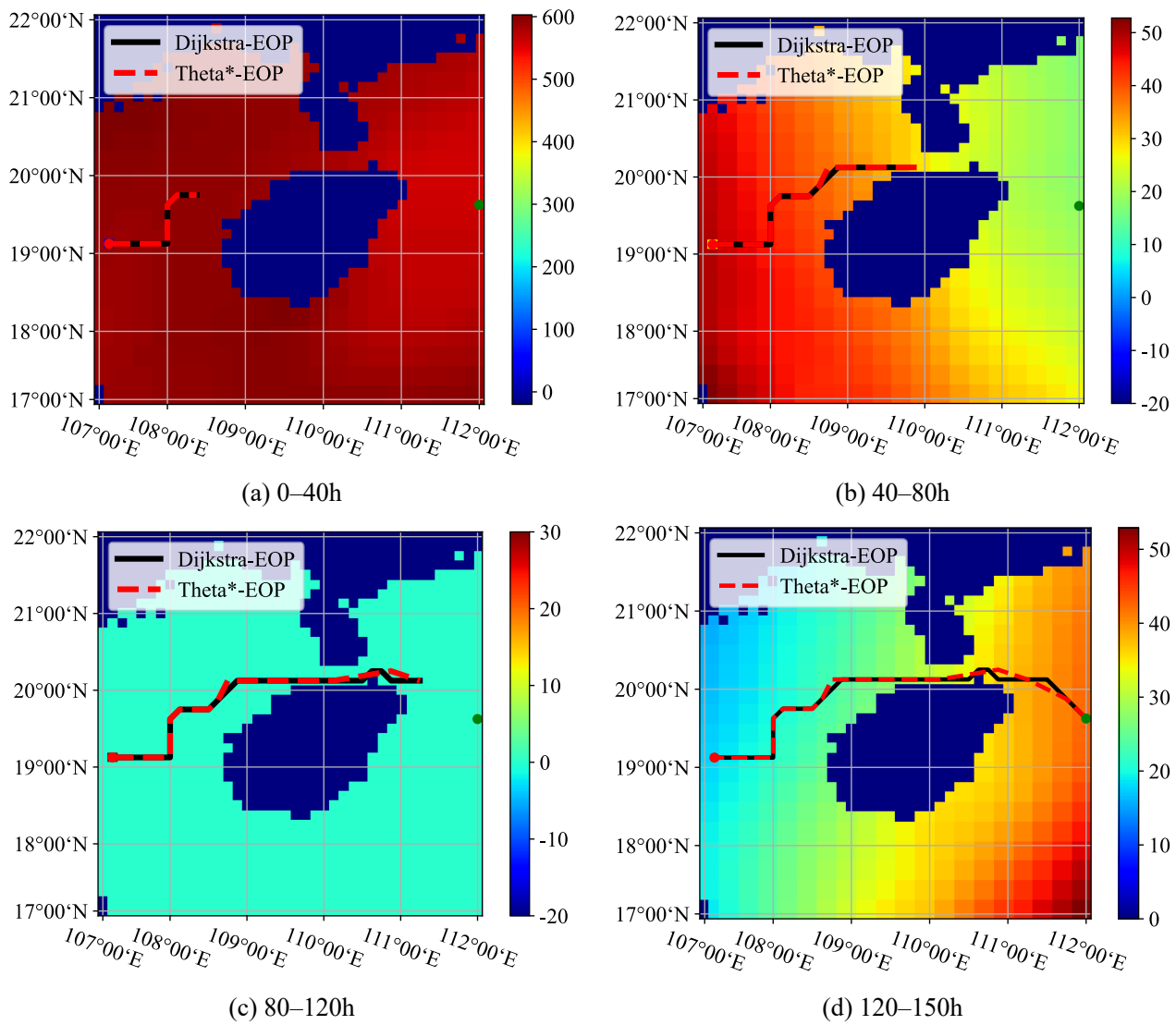
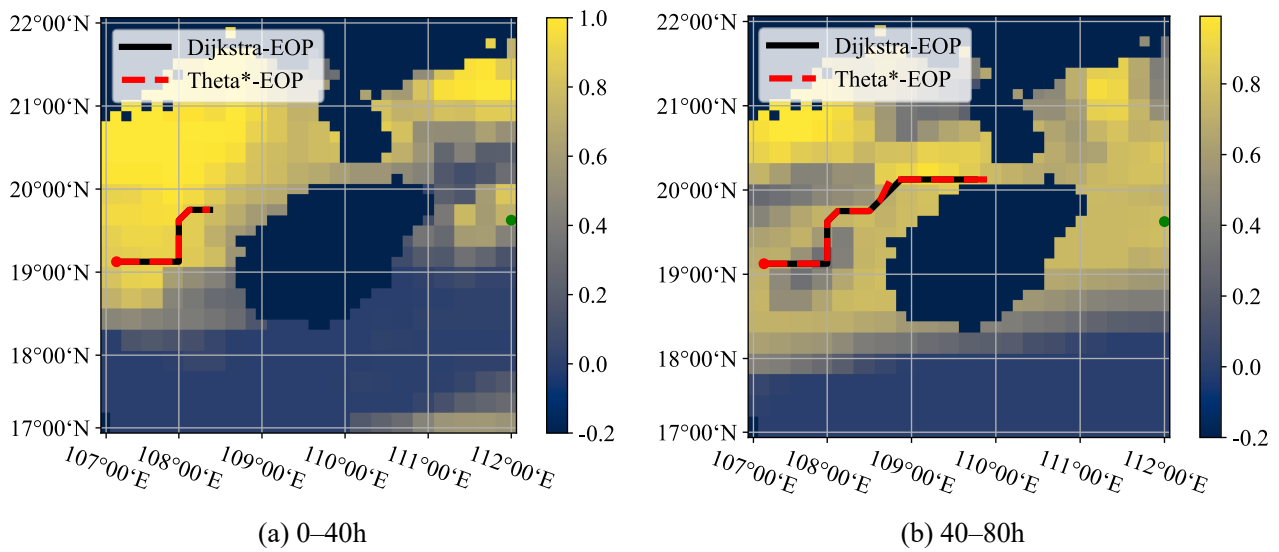
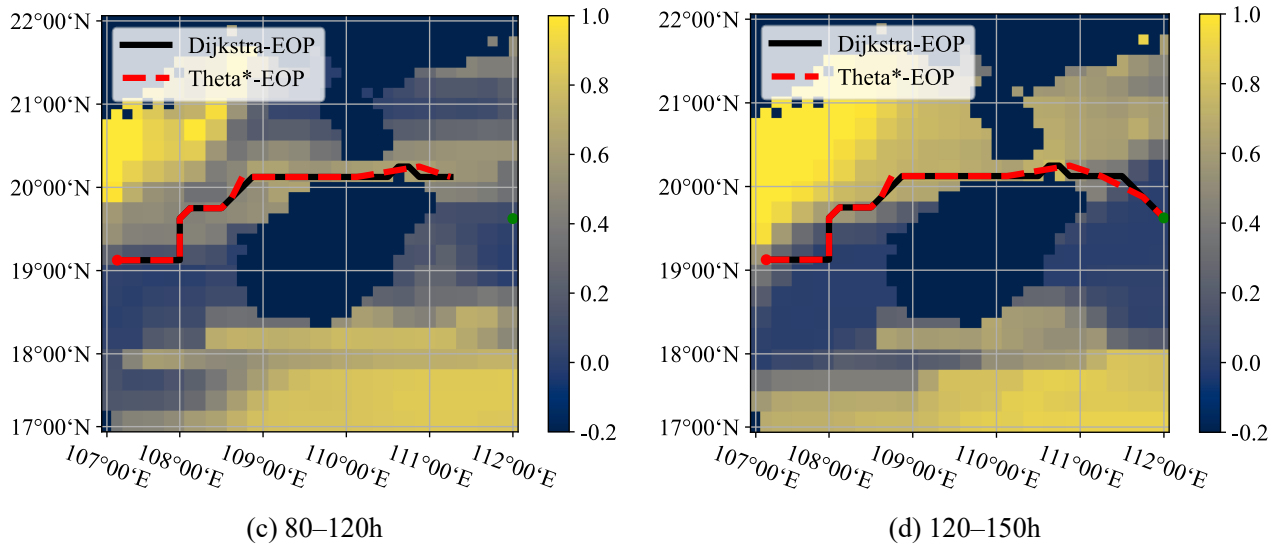


Fig. 16. Pathway in sea wind environment



**Fig .17.** Pathway in solar radiation environment





**Fig .18.** Pathway in atmospheric cloud environment

**Table 3**

Comparison of simulation results in dynamic ocean environment(case 1)

Method	path length (km)	Ocean capture capacity ( $\times 10^6\text{J}$ )	Wind capture capacity ( $\times 10^6\text{J}$ )	Solar capture capacity ( $\times 10^6\text{J}$ )	Total energy consumption ( $\times 10^6\text{J}$ )	Actual total energy consumption ( $\times 10^6\text{J}$ )	Navigation duration (h)	Energy consumption proportion (%)
Dijkstra	613.19	13.52	8.07	5.45	41.76	28.24	141.94	100.00
Dijkstra-EOP	621.39	13.7	8.22	5.48	37.09	23.39	143.84	82.83
Theta*	570.65	12.79	7.47	5.32	37.12	24.33	132.10	86.15
Theta*-EOP	582.68	13.71	8.12	5.59	36.39	22.68	134.87	80.31

In a dynamic and complex ocean environment, comparing the ocean energy capture, total energy consumption, and actual energy consumption of the four methods, it can be seen that the actual energy consumption of the Dijkstra EOP method is lower than that of the traditional Dijkstra method, and the proportion of energy consumption is reduced by 17.17%; The actual energy consumption of Theta\*-EOP method is lower than that of traditional Theta\* method, with a decrease of 5.84% in energy consumption; The actual energy consumption of Theta\*-EOP method is lower than that of Dijkstra EOP method, with a decrease of 2.52% in energy consumption.

In order to verify the effectiveness of the Theta\*-EOP algorithm, the start and target points were replaced, and the simulation results are shown in Figure 19 and Table 4.

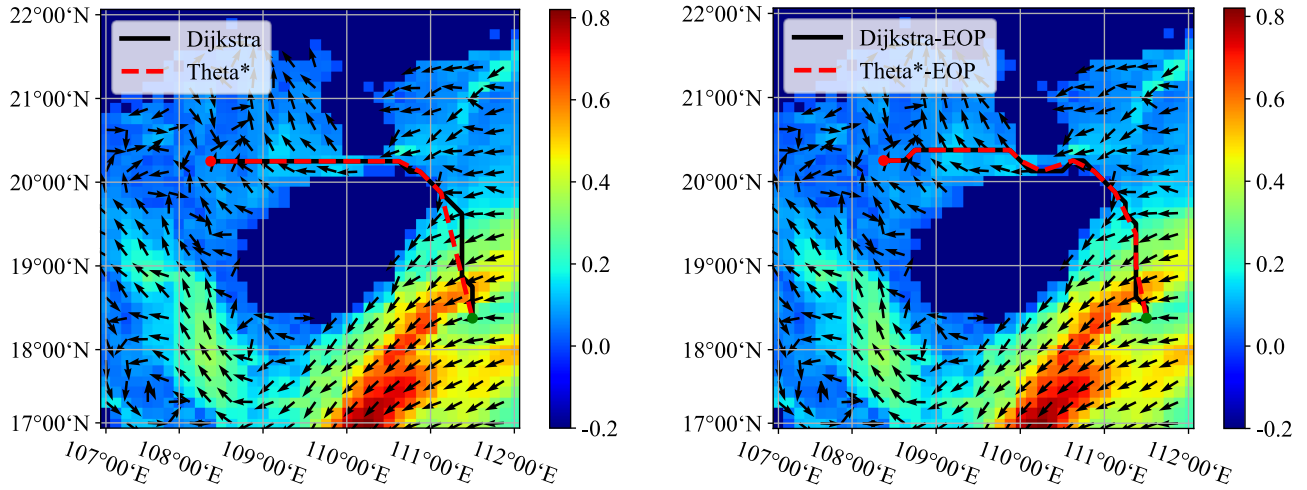


Fig .19. Pathway in ocean current environment

Table 4

Comparison of simulation results in dynamic ocean environment(case 2)

Method	path length (km)	Ocean capture capacity ( $\times 10^6\text{J}$ )	Wind capture capacity ( $\times 10^6\text{J}$ )	Solar capture capacity ( $\times 10^6\text{J}$ )	Total energy consumption ( $\times 10^6\text{J}$ )	Actual total energy consumption ( $\times 10^6\text{J}$ )	Navigation duration (h)	Energy consumption proportion (%)
Dijkstra	510.72	10.35	5.86	4.49	25.05	14.70	118.22	100.00
Dijkstra-EOP	533.96	10.56	5.89	4.67	24.27	13.71	123.60	93.27
Theta*	496.02	10.23	5.64	4.59	24.5	14.27	114.82	97.07
Theta*-EOP	516.04	10.47	5.72	4.75	23.97	13.50	119.45	91.84

From Table 4, it can be concluded that in a dynamic and complex marine environment, comparing the ocean energy capture, total energy consumption and actual energy consumption of the four methods, it can be seen that the actual energy consumption of the Dijkstra EOP method is lower than that of the traditional Dijkstra method, and the proportion of energy consumption is reduced by 6.73%. The actual energy consumption of the Theta\*-EOP method is lower than that of the traditional Theta\* method, which is reduced by 5.23%; The actual energy consumption of the Theta\*-EOP method is lower than that of the Dijkstra-EOP method, with a 1.43% reduction in energy consumption.

We can draw some conclusions by comparing the data in Table 3 and Table 4. After replacing the application example, the energy saving effect of the algorithm is reduced. The meaning of the application example is a variety of simulation experiments with different starting and target points. The paths for the two application examples of changing the start and target points are shown in Figures 15 and 19. In different application examples, the energy savings of Theta\*-EOP compared to Dijkstra were 19.69% (Table 3) and 8.16% (Table 4), respectively. However, despite the varying energy-saving effects of the algorithm in different examples, it is still capable of planning the path with the lowest actual energy consumption. Therefore, Theta\*-EOP has great application prospects and development space in the field of path planning considering energy.

By observing the wind and solar energy capture in Tables 3 and 4, it can be concluded that during the voyage, the proportion of wind energy captured is higher than that of solar energy. The reason for this phenomenon is that solar energy capture is influenced by the intensity of solar radiation and cloud cover, while wind energy capture is only affected by wind speed and direction. It should be noted that ocean currents act as a resistance during the voyage, and the role of the planning algorithm is to minimize this resistance effect.

In addition, it can be concluded from Table 2, 3 and 4 that the path length planned by Dijkstra-EOP and Theta\*-EOP is longer, however this is not unacceptable, and a longer path means that more energy can be captured, resulting in a lower net energy consumption. The reason for this is that Dijkstra-EOP and Theta\*-EOP plan the path with the goal of minimizing net energy consumption, rather than the shortest path length.

In fact, Through the above chart and related analysis, it is not difficult to find that the Theta\*-EOP algorithm still has shortcomings: (1) it does not maintain high energy-saving efficiency in every case; (2) it leads to a decrease in ocean energy capture; (3) it does not take into account the kinematic and dynamic constraints of OEDR. These are also the key research directions we will focus on in the future.

In summary, the Dijkstra EOP method and Theta\*-EOP method can fully consider the influence of dynamic and complex ocean environments on the energy consumption and ocean energy capture of the *Yulang*, and can also plan paths with less energy consumption compared to the traditional global path planning methods in dynamic ocean environments. Meanwhile, the Theta\*-EOP method has the best energy consumption ratio. From the point of view of the actual total energy consumption during the voyage, the Theta\*-EOP method has the best energy consumption ratio. Similarly, A has a lot of room for improvement.

## 5. Conclusion

Current research on energy-saving global path planning in the marine environment is overly reliant on idealized models of the ocean environment and does not adequately address the issue of multi-source marine energy capture. This paper addresses these research gaps by focusing on "Yulang" to study the problem of multi-energy capture path planning in dynamic marine environments, which is also the novelty of this paper. The main contributions of this paper are as follows:

(1) Using the raster method and data provided by the RTOFS and ECMWF systems, a dynamic raster marine environment model that includes ocean currents, sea breeze, solar radiation, and atmospheric clouds was established.

(2) Based on the energy consumption model and natural energy capture model of "Yulang," the cost function of the planning algorithm was improved. This cost function takes into account the capture of energy sources such as sea breeze and solar energy, as well as the energy consumption of each system in "Yulang."

(3) The impact of energy consumption is taken into account, and the concept of velocity stack is introduced, and the child node unfolding conditions of the Theta\*-EOP algorithm are improved. Due to the limited power of the thrusters, when the expansion of a sub-node incurs excessive energy consumption, the OEDUSV will not be able to reach the node. The line-of-sight method of the Theta\*-EOP algorithm was also improved. The line-of-sight method considers the effects of time changes, not just two-dimensional coordinates. This increases the applicability of the line-of-sight method.

Through the simulation experiments conducted, it can be concluded that the "Theta\*-EOP" algorithm can plan paths with lower energy consumption. Under the criterion of actual total energy consumption, the proposed Theta\*-EOP algorithm saves 19.69%(Case1,Table3) and 8.16%(Case2,Table4) compared to the Dijkstra algorithm respectively. Theta\*-EOP algorithm shows different energy-saving effects in different application cases, which shows that Theta\*-EOP algorithm still has great possibilities for improvement.

### CRedit authorship contribution statement

**Yulei Liao:** Methodology, Conceptualization, Funding acquisition. **Ke Li:** Validation, Visualization, Software. **Yongbo Zhao:** Visualization, Investigation, Resources, Writing – original draft. **Haotian Tang:** Supervision, Formal analysis, Writing – review & editing. **Xiaofeng Liu:** Data curation, Investigation. **Ming Zhang:** Writing – review & editing, Investigation. **Xiaofeng Liu:** Supervision, Investigation. **Zhi-Ming Yuan:** Writing – review & editing.

### Declaration of competing interest

The authors declare that they have no known competing financial interests or personal relationships that could have appeared to influence the work reported in this paper.

### Acknowledgements

This work was supported by the National Natural Science Foundation of China (Grant No. 52071097), the Fundamental Research Funds for the Central Universities (Grant No. 3072024XX0107), Stable Supporting Fund of National Key Laboratory of Autonomous Marine Vehicle Technology (Grant No. 2024-HYHXQ-WDZC01), Key Research and Development Program of Heilongjiang Province (Grant No.2022ZX01A05).

### References

- [1] Bai X, Li B, Xu X, et al. A Review of Current Research and Advances in Unmanned Surface Vehicles [J]. *Journal of Marine Science and Application*, 2022, 21(2): 47-58.
- [2] Shetty N B, Umesh P, Gangadharan K V. Multi-role Remotely Operated Marine Surface Vehicle [J]. *Journal of Marine Science and Application*, 2022, 21(3): 219-27.
- [3] Zhu W, Zhang L. Development of Unmanned Surface Vehicle [J]. *Marine Technology*, 2017, (02): 1-6.
- [4] Huang J-h, Liu H. A hybrid decomposition-boosting model for short-term multi-step solar radiation forecasting with NARX neural network [J]. *Journal of Central South University*, 2021, 28(2): 507-26.
- [5] Hu Y, Wang J. Study on Power Generation and Energy Storage System of a Solar Powered Autonomous Underwater Vehicle(SAUV); proceedings of the Energy Procedia, F 2012Apr 12-13, 2012 [C]. 2012.
- [6] Wang X M, Shang J Z, Luo Z R, et al. Reviews of power systems and environmental energy conversion for unmanned underwater vehicles [J]. *Renewable & Sustainable Energy Reviews*, 2012, 16(4): 1958-70.
- [7] Ma Z, Liu Y, Wang Y, et al. Improvement of Working Pattern for Thermal Underwater Glider; proceedings of the OCEANS Conference, Shanghai, PEOPLES R CHINA, F 2016Apr 10-13, 2016 [C]. 2016.
- [8] Jiang Q. Research on Disturbance Rejection control method of NSV Under the Influence of wind wave and current [D]; Harbin Engineering University, 2021.
- [9] Sun X, Sang H, Li C, et al. Research review on “Black Pearl” Wave Glider [J]. *Marine Sciences*, 2020, 44(12): 107-15.
- [10] Yu J, Sun Z, Zhang A. The Present Status of Environmental Energy Harvesting and Utilization Technology of Marine Robots [J]. *Robot*, 2018, 40(01): 89-101.
- [11] Yu J, Sun Z, Zhang A. Research Status and Prospect of Autonomous Sailboats [J]. *Research Status and Prospect of Autonomous Sailboats*, 2018, 54(24): 98-110.
- [12] Liao Y. Nonlinear Motion Control Methods of Unmanned Surface Vehicle [D]; Harbin Engineering University, 2012.
- [13] Liao Y, Wang L, Li Y, et al. Expression of Concern: The Intelligent Control System and Experiments for an Unmanned Wave Glider (Expression of Concern of Vol 11, art no E0168792, 2016) [J]. *Plos One*, 2022, 17(4).
- [14] Zhou H X, Cao J J, Fu J, et al. Swift: Transition Characterization and Motion Analysis of a Multimodal Underwater Vehicle [J]. *Ieee Robotics and Automation Letters*, 2024, 9(2): 1692-9.
- [15] Zhou H X, Xu H, Cao J J, et al. Robust adaptive control of underwater glider for bottom sitting-oriented soft landing [J]. *Ocean Engineering*, 2024, 293.
- [16] Ma Y, Zhao Y, Diao J, et al. Design of Sail-Assisted Unmanned Surface Vehicle Intelligent Control System [J]. *Mathematical Problems in Engineering*, 2016, 2016.
- [17] Xie L, Xue S, Zhang J, et al. A path planning approach based on multi-direction A\* algorithm for ships navigating within wind farm waters [J]. *Ocean Engineering*, 2019, 184: 311-22.

- [18] Lee H-Y, Shin H, Chae J. Path Planning for Mobile Agents Using a Genetic Algorithm with a Direction Guided Factor [J]. *Electronics*, 2018, 7(10).
- [19] Li K, Song Z, Liu X, et al. Optimal Energy Path Planning for Oceanic Energy-driven Vehicle [J]. *Unmanned Systems Technology*, 2022, 5(01): 51-9.
- [20] Cui Y, Ren J, Zhang Y. Path Planning Algorithm for Unmanned Surface Vehicle Based on Optimized Ant Colony Algorithm [J]. *Ieej Transactions on Electrical and Electronic Engineering*, 2022, 17(7): 1027-37.
- [21] Li P, Yan T, Yang S, et al. Energy-optimal Path Planning Algorithm for Unmanned Surface Vessel Based on Reinforcement Learning [J]. *Journal of Unmanned Undersea Systems*, 2023, 31(02): 237-43.
- [22] Gao M. Research on Path Planning of USV Considering Energy Consumption Optimization [D], 2022.
- [23] Xuan S, Xu Z, Sun S, et al. Path Planning of Unmanned Ship Based on the Tabu Search Algorithm [J]. *Ship Engineering*, 2022, 44(04): 8-13+37.
- [24] Niu H, Ji Z, Al S, et al. Energy efficient path planning for Unmanned Surface Vehicle in spatially-temporally variant environment [J]. *Ocean Engineering*, 2020, 196.
- [25] Zhang Y, Shi G, Liu J. Dynamic Energy-Efficient Path Planning of Unmanned Surface Vehicle under Time-Varying Current and Wind [J]. *Journal of Marine Science and Engineering*, 2022, 10(6).
- [26] Wu M, Zhang A, Gao M, et al. Ship Motion Planning for MASS Based on a Multi-Objective Optimization HA\* Algorithm in Complex Navigation Conditions [J]. *Journal of Marine Science and Engineering*, 2021, 9(10).
- [27] Lan W, Jin X, Wang T, et al. Improved RRT Algorithms to Solve Path Planning of Multi-Glider in Time-Varying Ocean Currents [J]. *Ieee Access*, 2021, 9: 158098-115.
- [28] Ma Y, Hu M Q, Yan X P. Multi-objective path planning for unmanned surface vehicle with currents effects [J]. *Isa Transactions*, 2018, 75: 137-56.
- [29] Jia Q, Liao Y, Xu P, et al. Long-Endurance Dynamic Path Planning Method of NSV Considering Wind Energy Capture [J]. *Journal of Marine Science and Engineering*, 2021, 9(8).
- [30] Jia Q, Liao Y, Pang S, et al. NSV long endurance path planning method considering wind energy capture [J]. *Journal of Central South University(Science and Technology)*, 2021, 52(09): 3212-22.
- [31] Li Z. Research on Dynamic Analysis and Energy Harvesting Coupling Design of Ocean Energy Driven Platform [D], 2021.
- [32] Jia Q, Liao Y, Xu P, et al. Modeling analysis and experiment for energy system of ocean energy driven unmanned marine vehicle: The Yulang II case study [J]. *Journal of Field Robotics*, 2024, 41(3): 735-65.
- [33] Li K. Research on the Method of Optimal Energy Path Planning of Natural Energy-Driven USV [D], 2022.
- [34] Liao Y, Li K, Zhao Y, et al. Energy Saving Local Path Planning for New Type of Ocean Robot Considering Energy Capture [J]. *Shipbuilding of China*, 2023, 64(06): 225-39.
- [35] Fang C, Zhang X, Yin J. Development status and trends of ocean forecasting system in the 21st Century [J]. *Marine Forecasts*, 2013, 30(04): 93-102.
- [36] Xia D, Ren X. Foreign ocean forecasting dynamics [J]. *Marine Forecasts*, 2012, 29(02): 73-4.
- [37] Wu Y, Wang Y, Jiang M, et al. Enlightenment on Building and Developing Ocean Observation Network of China from 2019 NOAA Science Report [J]. *Journal of Ocean Technology*, 2021, 40(03): 84-9.